Clinical & Experimental Immunology
The Journal of Translational Immunology

Clinical and Experimental Immunology ORIGINAL ARTICLE doi:10.1111/cei.12726

Intranasal immunization with heat shock protein 60 induces $CD4^+CD25^+GARP^+$ and type 1 regulatory T cells and inhibits early atherosclerosis

Y. Zhong,* H. Tang,† X. Wang,* Q. Zeng,* Y. Liu,* X.i Zhao,* K. Yu,* H. Shi,* R. Zhu* and X. Mao*
*Department of Cardiology, Institute of Cardiovascular Disease, Union Hospital, Tongji Medical College, Huazhong University of Science and Technology, and †Department of Pediatric Infectious and Immunological Diseases, Wuhan Children's Hospital, Wuhan, China

Accepted for publication 28 September 2015
Correspondence: Department of Cardiology, Institute of Cardiovascular Disease, Union Hospital, Tongji Medical College, Huazhong University of Science and Technology, Wuhan 430022, China.
E-mail: zyc811029@126.com; maoxiaobouh@126.com

Summary

Atherosclerosis is an autoimmune inflammatory disease involving both innate and adaptive immune mechanisms. Immune tolerance induction may have therapeutic potential for the suppression of atherosclerosis. Current interest is directed towards mucosal tolerance induction, especially nasal tolerance. Previous studies have shown that heat shock protein 60 (HSP60) is recognized as an important autoantigen in atherosclerosis, and nasal or oral HSP60 can induce tolerance and ameliorate atherosclerosis by inducing several subsets of regulatory T cells (T_{regs}) such as latency-associated peptide $(LAP)^+$ and forkhead box transcription factor 3 $(FoxP3)^+$ T_{regs}. However, little is known regarding the detailed mechanisms of nasal tolerance. Here, we again investigated the impact of nasal HSP60 on atherosclerosis and the mechanisms underlying the anti-atherosclerosis responses. We found that nasal HSP60 caused a significant 33·6% reduction in plaque size at the aortic root in the early stages of atherosclerosis ($P < 0{\cdot}001$). Notably, a significant increase in activated $CD4^+CD25^+$ glycoprotein A repetitions predominant $(GARP)^+$ T_{regs}, type 1 T_{regs} (Tr1 cells), and $CD4^+CD25^+FoxP3^+$ T_{regs}, as well as a marked decrease in the numbers of type 1 and 17 T helper cells was detected in the spleens and cervical lymph nodes of HSP60-treated mice. Moreover, nasal HSP60 increases the production of transforming growth factor (TGF)-β and interleukin (IL)-10 and decreases the secretion of IFN-γ and IL-17. Interestingly, the atheroprotective role of nasal HSP60 treatment was abrogated partly by the neutralization of IL-10. Our findings show that nasal administration of HSP60 can attenuate atherosclerotic formation by inducing $GARP^+$ T_{regs}, Tr1 cells and $FoxP3^+$ T_{regs}, and that these T_{regs} maintain immune homeostasis by secreting IL-10 and TGF-β.

Keywords: nasal tolerance, GARP, atherosclerosis, Regulatory T cells, inflammation

Introduction

The forkhead box transcription factor P3 (FoxP3) is particularly expressed in $CD4^+CD25^+$ T_{regs}, which are necessary and sufficient for the active suppression of immune responses against autoantigens and is essential for T_{reg} development and function [1–3]. However, several lines of evidence suggest that FoxP3 alone is not able to completely establish a stable regulatory phenotype, and its status as a genuine T_{reg} marker has been questioned [4–6]. Recently, glycoprotein-A repetitions predominant (GARP or LRRC32), a transmembrane protein with a large extracellular domain that contains 20 leucine-rich repeats, was found to be expressed specifically on the surface of activated human T_{regs} and to play a crucial role in T_{reg} suppression [7,8]. Importantly, GARP has been identified as a receptor for latency-associated peptide (LAP), which requires transforming growth factor (TGF)-β for binding to GARP [9,10]. Furthermore, a positive feedback loop between GARP and FoxP3 is present in human T_{regs} [11]. Emerging experimental evidence suggests that several subsets of T_{regs}, including $FoxP3^+$ T_{regs}, LAP^+ T_{regs} and type 1 T_{regs} (Tr1 cells), can inhibit autoimmunity in animal models of inflammatory and autoimmune diseases [12–14], particularly atherosclerosis [15,16], through the down-regulation

of activated T cell responses. In a recent study, we found that the frequency and function of circulating $CD4^+CD25^+GARP^+$ T_{regs} were down-regulated in patients with acute coronary syndrome, suggesting that GARP may promote the protective function of T_{regs} in atherosclerotic disease [17].

The autoimmune concept of atherosclerosis was first presented by Wick *et al.* in 1992, and has since been proven in a large number of experimental and clinical studies [18]; according to this idea, cells of the innate and adaptive immune system, especially activated $CD4^+$ T cells, may be involved in the initiation and progression of atherosclerosis [19–21]. HSP60, a member of the highly conserved heat shock protein (HSP) family, can be considered an important antigenic determinant of autoantibodies that participates in several autoimmune diseases, in particular atherosclerosis [22–24]. Previous studies have shown enhanced HSP60 expression in human atherosclerotic plaques [25]. Recently, Xu *et al.* and Zhang *et al.* reported that elevated titres of HSP60-specific antibodies can be found in the serum of patients with atherosclerosis [26,27]. Additionally, activated $CD4^+$ T cells that react specifically to self-HSP60 peptides have been detected in carotid plaques of atherosclerosis patients, suggesting that HSP60-reactive $CD4^+$ T cells contribute to the autoimmune reactions in atherosclerosis [28]. This autoimmune process may be related to an existing deficit in immunological tolerance and dampened by activated T_{regs}. Accumulating evidence has shown that mucosal administration of autoantigens such as HSPs, oxidized low-density lipoprotein (ox-LDL) and glycoproteins could induce immune tolerance, resulting in increased numbers of several subsets of T_{regs} and decreased atherosclerotic plaque area [28–33].

Currently, two principal routes of mucosal tolerance induction are known: oral and nasal. Several previous studies have demonstrated that administering low doses of antigens orally induces many types of antigen-specific T_{regs}, including $CD4^+CD25^+FoxP3^+$ T_{regs}, T helper type 3 (Th3) cells, Tr1 cells and $CD4^+LAP^+$ T_{regs}, indicating that oral tolerance induction is an effective method for treating autoimmune diseases such as atherosclerotic disease [15,33,34]. Simultaneously, nasal tolerance induction has been shown to be as effective as immune tolerance induced via the oral route in inhibiting autoimmune diseases; furthermore, the nasal route requires substantially lower doses of antigen than the oral route [35,36]. Recently, we found that nasal administration of low doses of ox-LDL inhibits the development of atherosclerosis through a significant increase in $CD4^+CD25^+FoxP3^+$ and $CD4^+LAP^+$ T_{regs}, which can suppress immune responses due to types 1, 2, and 17 T helper cells [33]. In addition, our experimental groups also indicated that $CD4^+CD25^+FoxP3^+$ and $CD4^+LAP^+$ T_{regs} induced by nasal HSP60 may be relevant to the suppression of atherosclerosis [32]. However, as yet it remains uncertain whether nasal administration of HSP60 could induce other subsets of T_{regs}, such as $CD4^+CD25^+GARP^+$ T_{regs} and Tr1 cells.

In the present study, we again show that nasal administration of HSP60 significantly attenuated early atherosclerosis in apolipoprotein E $(ApoE)^{-/-}$ mice and was associated with the induction of several types of T_{reg} populations, including $CD4^+CD25^+GARP^+$ T_{regs}, Tr1 cells and $CD4^+CD25^+FoxP3^+$ T_{regs}, which suppressed T helper type 1 (Th1) and Th17 cell immune responses.

Methods

Animals

Six-week-old male $ApoE^{-/-}$ mice from a C57BL/6J background (Jackson Laboratory, Bar Harbor, ME, USA) were bred and maintained in the Animal Center at Beijing University. The mice were kept in a specific pathogen-free facility (Tongji Medical College, Wuhan, China) and were given a western-type diet containing 0·15% cholesterol and 21% fat. The mice were fed a normal chow diet during nasal HSP60 or phosphate-buffered saline (PBS) treatment. All experiments were performed according to the guidelines for the Care and Use of Laboratory Animals (Science and Technology Department of Hubei Province, China, 2005). The protocol was approved by the Animal Care and Use Committee of Hubei Province.

Experimental groupings

Six- and 16-week-old male mice were nasally administered 15 μl of PBS (pH 7·4) or 3 μg of HSP60 dissolved in 15 μl PBS by a micropipette once daily for 5 consecutive days ($n = 6$ for each group). At 16 and 24 weeks of age, the mice were killed by cervical dislocation and the atherosclerotic plaques were evaluated. For the interleukin (IL)-10 blocking experiment, 6-week-old mice ($n = 6$) were administered 3 μg of HSP60 nasally once daily for 5 consecutive days. Subsequently, these mice were injected intraperitoneally once weekly with 100 μg of neutralizing anti-interleukin (IL)-10 antibody from 7 to 16 weeks of age [33,37], after which atherosclerotic plaques were evaluated. Control mice ($n = 6$) were treated with equal amounts of rat immunoglobulin (Ig)G.

Reagents and antibodies

Recombinant *Helicobacter pylori* HSP60 was obtained from Shanghai Linc-Bio Science Co. Ltd (Shanghai, China). Anti-CD4-fluorescein isothiocyanate (FITC) monoclonal antibody (mAb) (Cat. no.11-0041), anti-CD25-phycoerythrin (PE) mAb (Cat. no. 12-0251), anti-FoxP3-allophycocyanin (APC) mAb (Cat. no. 88-8118), anti-interferon (IFN)-γ-PE mAb (Cat no. 12-7311), anti-IL-4-PE mAb (Cat. no. 12-7041), anti-IL-17A-PE mAb (Cat. no. 12-7177), anti-CD3 mAb (Cat no. 14-0032), anti-CD28

mAb (Cat. no. 14-0281), anti-GARP-APC mAb (Cat. no. 17-9891), anti-IgG_1-APC mAb (Cat. no. 17-4714) and anti-IgG_1-PE mAb (Cat. no. 12-4714) were purchased from eBioscience (San Diego, CA, USA). Anti-IL-10Rβ-APC mAb (Cat. no. FAB5368A), anti-IFN-γR_1-PE mAb (Cat. no. FAB1026P), anti-IL-10 mAb (Cat. no. MAB417) and control rat IgG (Cat. no. 6-001-A) were obtained from R&D Systems (Minneapolis, MN, USA).

Serum total cholesterol levels

After clotting at room temperature, serum was obtained from experimental and control group mice via centrifugation at 1200 ***g*** for 10 min and stored at −80°C. Total cholesterol levels were measured as described in detail previously [33].

Atherosclerotic plaque analysis

Mice were killed at 16 and 24 weeks of age, and the aortic root plaques were assessed. After removal of the blood residue, the aortas were quickly dissected and removed from the higher region of the aortic sinus to the lower region of the left and right iliac artery. In addition, we retained the heart with the aortic sinus, as well as spleens and cervical lymph nodes (CLNs), which were routinely considered the nose-draining lymphatic nodes [33,38]. For plaque analysis, the hearts with the aortic root were embedded in optimal cutting temperature (OCT) compound for frozen tissue sectioning. Six consecutive cryosections (10-μm thickness) with three aortic valves were obtained from the aortic root of each mouse and stained with oil red O and haematoxylin for lipid visualization. All slices were collected on a Leica CM 1850 Cryostat (Leica Microsystems, Wetzlar, Germany). Plaque area was calculated using Image-Pro Plus version 6·0 software (Media Cybernetics, Rockville, MD, USA).

Flow cytometry analysis

At the days 4 and 14 after the final nasal administration, splenocytes and CLN cells were harvested from HSP60-treated mice ($n = 6$ for each group). Untreated mice ($n = 6$) were used as controls. The monocytes were suspended and cultured as described previously [33]. For GARP induction, the cells (2×10^6/sample) were stimulated with soluble anti-CD3 mAb (1·5 μg/ml) and anti-CD28 mAb (2 μg/ml) at 37°C with 5% CO_2 for 24 h, and the cells were subsequently harvested for staining.

T_{regs} were analysed as follows: (1) for the detection of $CD4^+CD25^+GARP^+$ T_{regs}, the cells were stained with anti-GARP-APC, anti-CD4-FITC and anti-CD25-PE mAb, as described previously [17]; (2) for the detection of $CD4^+$ IFN-γR^+ IL-$10R^+$ T_{regs} (Tr1), the cells were stained with anti-IFN-γR1-PE, anti-IL-10Rβ-APC and anti-CD4-FITC mAb as described previously [39]; and (3) for the detection of $CD4^+CD25^+FoxP3^+$ T_{regs}, the cells were stained as described previously [33].

For the analysis of $CD4^+$IFN-γ^+ (Th1), $CD4^+$IL-4^+ (Th2) and $CD4^+$IL-17^+ (Th17) T cells, the cells were stimulated with phorbol myristate acetate (PMA, 20 ng/ml) plus ionomycin (1 μg/ml; Alexis Biochemicals, San Diego, CA, USA) for 4 h in the presence of 2 μmol/ml monensin (Alexis Biochemicals). The incubator was set at 37°C under a 5% CO_2 environment. After 4 h of culture, the monocytes were collected for staining with anti-CD4-FITC mAb according to the manufacturer's instructions. Fixation and permeabilization were necessary before staining with anti-IFN-γ-PE, anti-IL-4-PE or anti-IL-17-PE mAb.

Isotype-specific controls were given to enable correct compensation and to validate antibody specificity. All stained cells were analysed immediately by flow cytometry using a fluorescence activated cell sorter (FACS)Calibur (BD Biosciences), and all data were analysed using the FlowJo 7·6·1 software program (TreeStar Inc., Ashland, OR, USA).

Responder T cells and T_{reg} co-culture

On day 14 after the last nasal administration, $CD4^+$ T cells were isolated from pooled splenocytes of HSP60- or PBS-treated mice using a $CD4^+$ T cell-positive isolation Kit II (Miltenyi Biotec, Gladbach, Germany). The purified $CD4^+$ T cells were stained with anti-GARP-APC, anti-CD4-FITC and anti-CD25-PE mAb for 30 min at 4°C. Responder T cells (T_{resps}, $CD4^+CD25^-GARP^-$ T cells) and $CD4^+CD25^+GARP^+$ T_{regs} were isolated by FACS. The purity of the sorted population was > 93% using FACS analysis. The T_{regs} and T_{resps} were divided into two groups: (1) $CD4^+CD25^+GARP^+$ T_{regs} (1×10^4 cells/well) were stimulated with concanavalin A (ConA) *in vitro* for 72 h, and the supernatants were collected for detecting the anti-inflammatory cytokines IL-10 and TGF-β1; (2) purified $CD4^+CD25^+GARP^+$ T_{regs} were co-cultured with $CD4^+$ $CD25^-GARP^-$ T cells (5×10^3 cells/well) at different ratios (T_{regs}/T_{resps} ratios: 1 : 1, 1 : 2, 1 : 4 and 1 : 8) as described previously [17]. The inhibitory effects were measured using an MTT assay. MTT (20 μl of 5 mg/ml) was added to each well 4 h prior to harvest. The supernatant in each well was removed, and 150 μl of DMSO was added and stirred for 10 min. The absorbance (A) values were determined at 570 nm on a microplate reader. Dulbecco's modified Eagle's medium (DMEM)-F12 culture medium was used as blank control in the normal control group and for zero adjustment of the microplate reader. All measurements were performed in triplicate. The rate of cell proliferation was calculated as follows: cell proliferation rate = (A value in test group – A value in normal control group)/A value in normal control group × 100%.

Table 1. Sequences of primers for real-time reverse transcription–polymerase chain reaction (RT–PCR)

Molecule	Sequence (5'–3')
IFN-γ sense	CGGCACAGTCATTGAAAGCCTA
IFN-γ anti-sense	GTTGCTGATGGCCTGATTGTC
IL-4 sense	TCTCGAATGTACCAGGAGCCATATC
IL-4 anti-sense	AGCACCTTGGAAGCCCTACAGA
IL-10 sense	GACCAGCTGGACAACATACTGCTAA
IL-10 anti-sense	GATAAGGCTTGGCAACCCAAGTAA
IL-17 sense	TCTCTGATGCTGTTGCTGCT
IL-17 anti-sense	CGTGGAACGGTTGAGGTAGT
TGF-β sense	GTGTGGAGCAACATGTGGAACTCTA
TGF-β anti-sense	TTGGTTCAGCCACTGCCGTA
CD25 sense	CTGATCCCATGTGCCAGGAA
CD25 anti-sense	AGGGCTTTGAATGTGGCATTG
Foxp3 sense	CTCATGATAGTGCCTGTGTCCTCAA
Foxp3 anti-sense	AGGGCCAGCATAGGTGCAAG
GARP sense	ACCTCCACAGCAATGTCCTC
GARP anti-sense	TGCTGTTGCAGCTCAAGTCT
VCAM-1 sense	CCTCACTTGCAGCACTACGGGCT
VCAM-1 anti-sense	TTTTCCAATATCCTCAATGACGGG
MCP-1 sense	TTCCTCCACCACCATGCAG
MCP-1 anti-sense	CCAGCCGGCAACTGTGA
GAPDH sense	ACCACAGTCCATGCCATCAC
GAPDH anti-sense	TCCACCACCCTGTTGCTGTA

Enzyme-linked immunosorbent assay (ELISA)

At the days 4 and 14 and weeks 8 and 16 after the last administration, splenocytes were isolated and cultured with ConA. Untreated or PBS-treated mice were used as controls. The IFN-γ, IL-4, IL-17, TGF-β1 and IL-10 levels in the supernatants were quantified using ELISA kits (eBioscience). In addition, as mentioned above, the levels of IL-10 and TGF-β1 in the $CD4^+CD25^+GARP^+$ T_{reg} culture supernatant were measured by ELISA. All procedures were conducted following the manufacturer's instructions. All samples were measured in duplicate.

Real-time reverse transcription–polymerase chain reaction (RT–PCR)

Total RNA from splenocytes and the descending aortas was prepared using RNAiso Plus (Takara Biotechnology, Shiga, Japan). cDNA was transcribed from purified RNA using a RNA PCR kit (Takara Biotechnology). Real-time PCR was performed as described previously [33]. The primers are indicated in Table 1.

Statistical analysis

All statistical analyses were performed using SPSS version 17·0. The results are expressed as the mean ± standard deviation (s.d.). One-way analysis of variance (ANOVA) was used for multiple comparisons, followed by the Newman–Keuls test. Differences were considered significant at $P < 0{\cdot}05$.

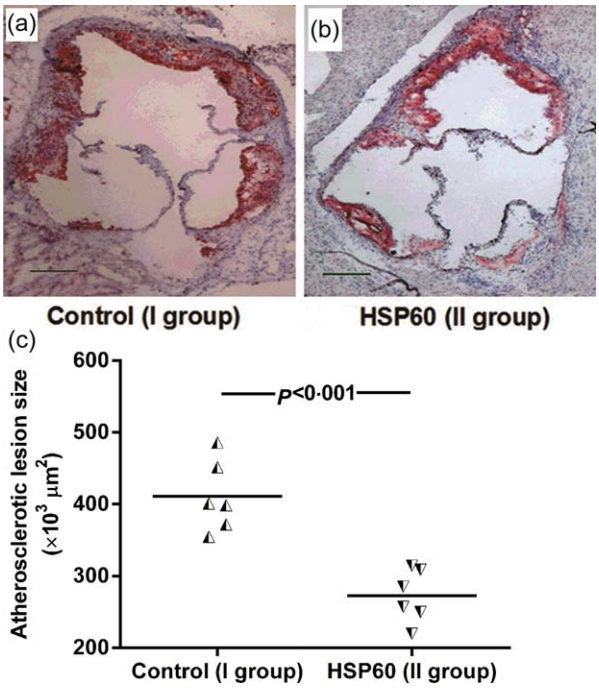

Fig. 1. Nasal heat shock protein (HSP)60 inhibits atherosclerotic lesion formation. (a) and (b) representative photomicrographs of oil red O- and haematoxylin-stained aortic root sections from the phosphate-buffered saline (PBS)-treated group ($n = 6$) and the HSP60-treated group ($n = 6$), respectively. (c) The data from two groups are shown: the half black regular triangles represent animals from the PBS-treated group, and the half black inverted triangles represent animals from the HSP60-treated group. A black bar represents 200 μm. The horizontal bars represent the means.

Results

Nasal HSP60 inhibits early atherosclerosis in $ApoE^{-/-}$ mice

To determine the influence of nasal induction of HSP60 tolerance on atherosclerosis initiation, atherosclerosis was induced after the nasal administration of PBS (group I) or HSP60 (group II) for 5 consecutive days to $ApoE^{-/-}$ mice. Mice were placed subsequently on a western-type diet for 10 weeks, and then atherosclerotic plaque formation was analysed in oil red O and haematoxylin-stained cryosections of the aortic root. Interestingly, the atherosclerotic plaque size in the aortic root was reduced significantly (33·6% reduction) in mice treated with HSP60 compared with PBS-treated mice (272 645·6 ± 30 346·6 μm^2 *versus* 410 687.7 ± 38 708·4 μm^2, respectively; $P < 0{\cdot}001$; Fig. 1). In addition, the influence of nasal HSP60 on atherosclerosis progression was evaluated. Six-week-old $ApoE^{-/-}$ mice were fed a western-type diet for 10 weeks to induce atherosclerotic plaque formation in the aortic root. Then, these mice were administered nasally with PBS (group III) or HSP60 (group IV) for 5 consecutive days and subsequently

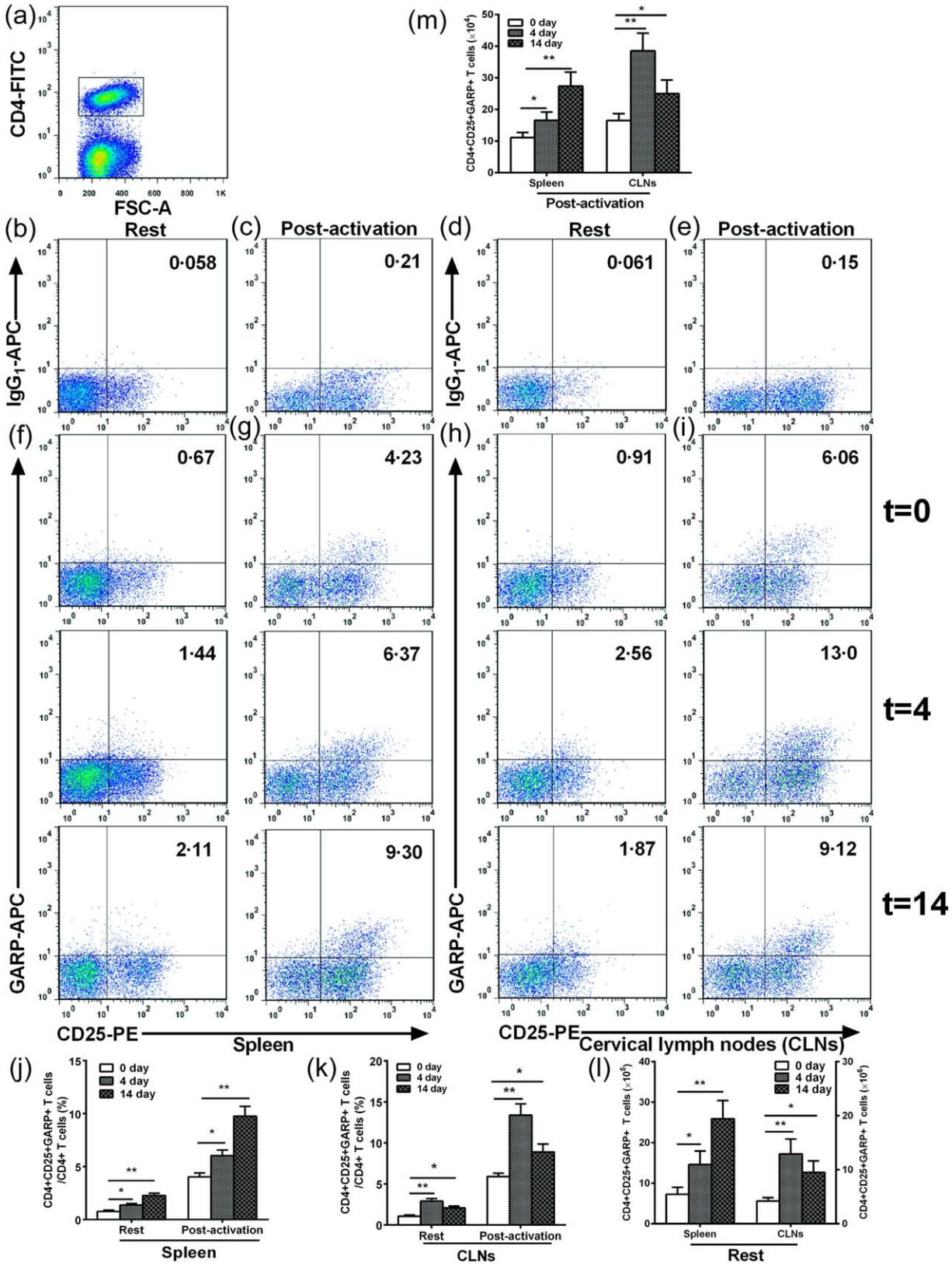

Fig. 2. Effects of nasal heat shock protein (HSP)60 on $CD4^+CD25^+GARP^+$ regulatory T cells (T_{regs}) in spleens and cervical lymph nodes (CLNs). Apolipoprotein E $(ApoE)^{-/-}$ mice were nasally administered HSP60 for 5 days and were killed 4 and 14 days after the final nasal treatment. Untreated mice ($t = 0$) were considered controls. For glycoprotein A repetitions predominant (GARP) activation, the cells (2×10^6/sample) were stimulated with soluble anti-CD3 monoclonal antibody (mAb) (1·5 μg/ml) and anti-CD28 mAb (2 μg/ml) at 37°C with 5% CO_2 for 24 h. (a) $CD4^+$ T cell subsets were gated. (b–e) Representative results for isotype controls in spleens and CLNs estimated by fluorescence activated cell sorter (FACS) analysis. (f–i) Representative results for unstimulated and stimulated $CD4^+CD25^+GARP^+$ T_{regs} in spleens and CLNs estimated by FACS analysis. (j,k) The graphs represent the percentage of unstimulated and stimulated $CD4^+CD25^+GARP^+$ T_{regs} in spleens and CLNs. (l,m) The graphs represent the absolute number of unstimulated and stimulated $CD4^+CD25^+GARP^+$ T_{regs} in spleens and CLNs. $^*P < 0{\cdot}05$, $^{**}P < 0{\cdot}01$. The data are expressed as the mean ± standard error of the mean (s.e.m.) and are representative of at least three independent experiments.

fed a western-type diet for another 7 weeks. At 24 weeks, the mice were euthanized and atherosclerotic plaques were calculated. However, only a mild but not statistically significant reduction was found in group IV compared with group III (Supporting information, Fig. S1a,b,d). To develop an effective approach for inhibiting atherosclerosis progression, we carried out another animal experiment. On the basis of group IV, mice were treated nasally with 3 μg of HSP60 (group V) once weekly from 18 to 24 weeks and then euthanized. Unfortunately, only a trend of an 11·3% decrease in atherosclerotic plaque size was found in group V compared with group III, and no significant differences were observed (Supporting information, Fig.S1c,b,d). As expected, nasal HSP60 did not change body weight or total serum cholesterol levels significantly, in agreement with our previous findings (Supporting information, Table S1) [32,33].

Nasal HSP60 induces $CD4^+CD25^+GARP^+$ T_{regs} in spleens and CLNs

We investigated whether nasal HSP60 atheroprotection was dependent on the induction of $CD4^+CD25^+GARP^+$ T_{regs}, which were detected on days 4 and 14 after the final nasal treatment, consistent with our previous studies [32,33]. As shown in Fig. 2, we found that the frequency of $CD4^+CD25^+GARP^+$ T_{regs} present in untreated mice was 0·77 ± 0·12% in spleens and 1·07 ± 0·14% in CLNs. Surprisingly, the frequency of $CD4^+CD25^+GARP^+$ T_{regs} increased markedly to 1·37 ± 0·14% in the spleens and 2·90 ± 0·32% in the CLNs of HSP60-treated mice on day 4 and to 2·28 ± 0.20% in spleens and 2·07 ± 0·22% in CLNs on day 14 when compared with untreated mice (Fig. 2f,h,j,k; all $P < 0{\cdot}05$). Furthermore, absolute numbers of $CD4^+CD25^+GARP^+$ T_{regs} were also increased in the spleens and CLNs of HSP60-treated mice (Fig. 2l, all $P < 0{\cdot}05$). Increasing evidence has implicated GARP as a specific marker of activated T_{regs} [8–10]. Therefore, we next measured the frequency of activated $CD4^+CD25^+GARP^+$ T_{regs} after 24 h of T cell receptor (TCR) stimulation with anti-CD3 mAb and anti-CD28 mAb, which were used to activate immunocytes because of its high specificity and properties of physiological stimulation. Our data showed that the frequency of activated $CD4^+CD25^+GARP^+$ T_{regs} was significantly higher than observed under resting conditions in all the groups examined. Interestingly, there was a significant increase in the frequency of activated $CD4^+CD25^+GARP^+$ T_{regs} in the spleens and CLNs of HSP60-treated mice on day 4 (HSP60-treated mice *versus* untreated mice; 6·08 ± 0·54% *versus* 4·01 ± 0·38% in spleens, $P < 0{\cdot}05$; 13·37 ± 1·39% *versus* 5·90 ± 0·40% in CLNs, $P < 0{\cdot}05$; Fig. 2g, i–k) and day 14 compared with untreated mice (HSP60-treated mice *versus* untreated mice; 9·74 ± 0·92% *versus* 4·01 ± 0·38% in spleens, $P < 0{\cdot}05$; 8·89 ± 0·97% *versus* 5·90 ± 0·40% in CLNs, $P < 0{\cdot}05$; Fig. 2g, i–k).

Furthermore, we also investigated whether nasal HSP60 affects the suppressive function of activated $CD4^+CD25^+GARP^+$ T_{regs}. Our data indicated that the suppressive function of activated $CD4^+CD25^+GARP^+$ T_{regs} was not remarkably altered by nasal HSP60 using *in-vitro* suppression assays (Supporting information, Fig. S2). In addition, we examined anti-inflammatory cytokine

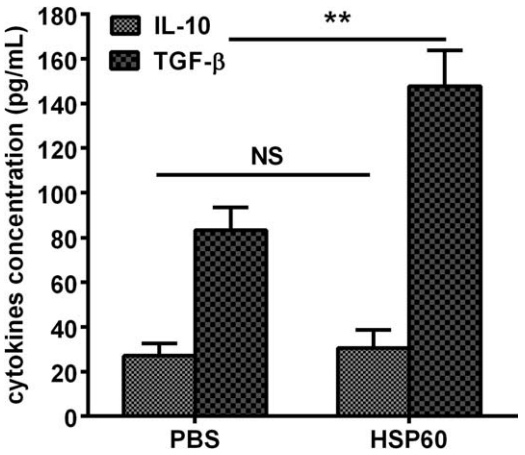

Fig. 3. Effects of nasal heat shock protein (HSP)60 on transforming growth factor (TGF)-β and interleukin (IL)-10 production in $CD4^+CD25^+$ glycoprotein A repetitions predominant $(GARP)^+$ regulatory T cells (T_{regs}). $CD4^+CD25^+GARP^+$ T_{regs} isolated from spleens on the day 14 after the final nasal HSP60 and phosphate-buffered saline (PBS) treatments were stimulated with concanavalin A (ConA) *in vitro* for 72 h. TGF-β and IL-10 production was detected in the supernatants. $^{**}P < 0{\cdot}01$. The data are expressed as the mean ± standard error of the mean (s.e.m.) and are representative of at least three independent experiments.

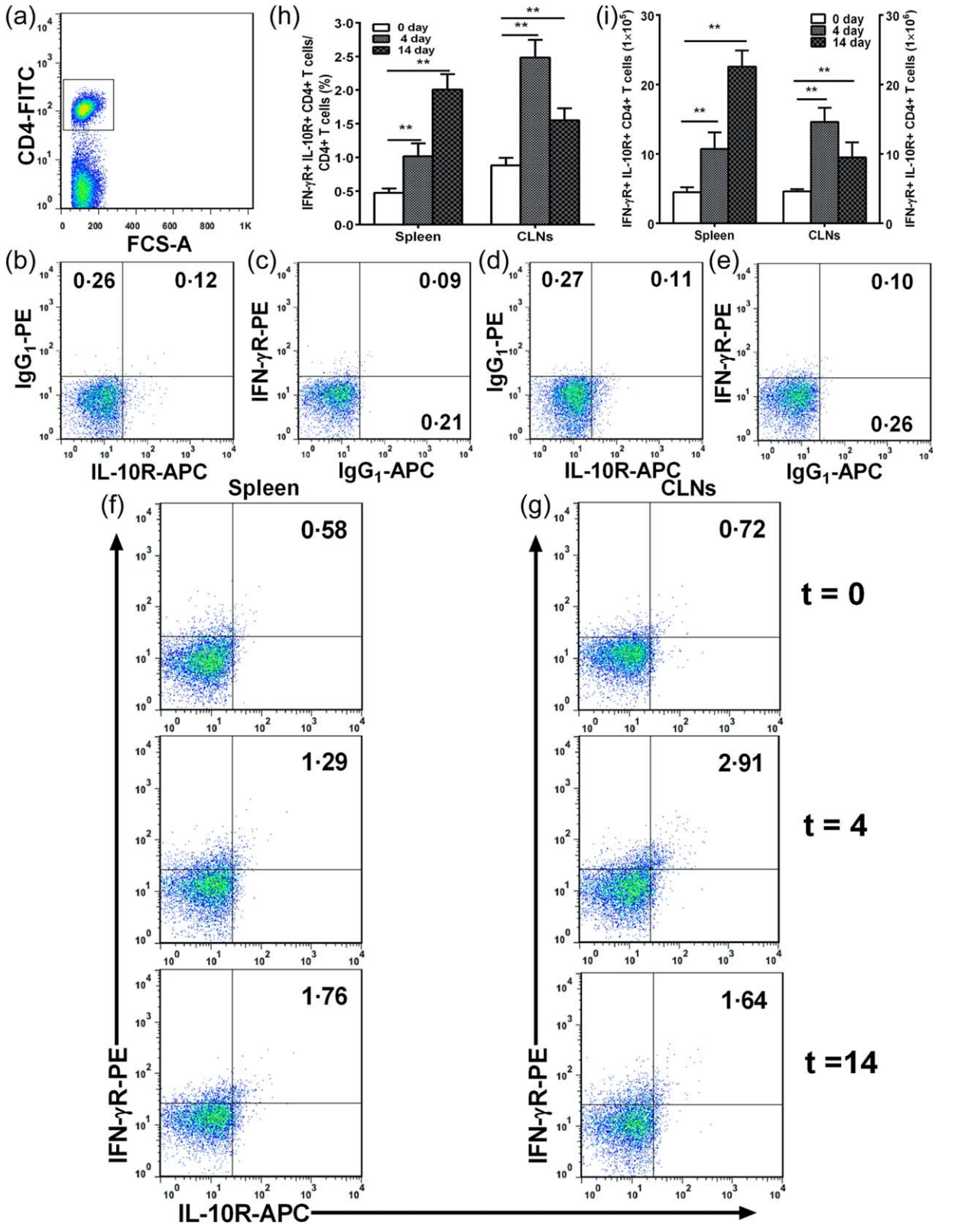

production from $CD4^+CD25^+GARP^+$ T_{regs} in response to ConA, which was a polyclonal stimulant and exhibited a more powerful effect than anti-CD3 mAb and anti-CD28 mAb. The most exciting implications are that a significant up-regulation of TGF-β secreted by $CD4^+CD25^+GARP^+$ T_{regs} was observed in HSP60-treated mice compared with

Fig. 4. Effects of nasal heat shock protein (HSP)60 on $CD4^+$interleukin (IL)$-10R^+$interferon (IFN)-γR^+ regulatory T cells (T_{regs}) (Tr1) in spleens and cervical lymph nodes (CLNs). Apolipoprotein E $(ApoE)^{-/-}$ mice were administered nasally HSP60 for 5 days and were killed 4 and 14 days after the final nasal treatment. Untreated mice ($t = 0$) were considered controls. (a) $CD4^+$ T cell subsets were gated. (b–e) Representative results for isotype controls in spleens and CLNs estimated by fluorescence activated cell sorter (FACS) analysis. (f,g) Representative results for type 1 T_{regs} (Tr1) cells in spleens and CLNs estimated by fluorescence activated cell sorter (FACS) analysis. (h) The graphs represent the percentage of Tr1 cells in spleens and CLNs. (i) The graphs represent the absolute number of Tr1 cells in spleens and CLNs. $^{**}P < 0{\cdot}01$. The data are expressed as the mean ± standard error of the mean (s.e.m.) and are representative of at least three independent experiments.

PBS-treated mice (147·7 ± 10·4 pg/ml *versus* 83·1 ± 10·4 pg/ml, $P < 0{\cdot}01$; Fig. 3). Nevertheless, the levels of IL-10 were similar in the supernatants of $CD4^+CD25^+GARP^+$ T_{regs} between HSP60-treated and PBS-treated mice (Fig. 3).

Nasal HSP60 induces Tr1 and $CD4^+CD25^+FoxP3^+$ T_{regs} in spleens and CLNs

Next, we evaluated the effect of nasal induction of HSP60 tolerance on Tr1 and $CD4^+CD25^+FoxP3^+$ T_{regs}. When compared with untreated mice (0·48 ± 0·05% in spleens, 0·88 ± 0·09% in CLNs; Fig. 4d), the frequency of Tr1 cells was up-regulated significantly to 1·02 ± 0·16% and 2·01 ± 0·17% in spleens (all $P < 0{\cdot}01$; Fig. 4f,h) and 2·48 ± 0·20% and 1·55 ± 0·14% in CLNs (all $P < 0{\cdot}01$; Fig. 4g,h) on days 4 and 14 after the final nasal treatment, respectively. Interestingly, absolute numbers of Tr1 cells were also up-regulated in the spleens and CLNs of HSP60-treated mice, respectively (Fig. 4i, all $P < 0{\cdot}01$). Similar to our previous report [32,33], we also found a significant increase in the frequency and number of $CD4^+CD25^+FoxP3^+$ T_{regs} in the spleens and CLNs of HSP60-treated mice on days 4 and 14 compared to untreated mice, respectively (data not shown).

Nasal HSP60 suppresses Th1 and Th17 cells in spleens and CLNs

Furthermore, we examined whether nasal HSP60 affected Th1, Th2 and Th17 cells in spleens and CLNs. We observed a significant reduction in the frequency of Th1 cells in the spleens and CLNs of HSP60-treated mice on days 4 and 14 compared with untreated mice (untreated mice *versus* HSP60-treated mice on day 4 and *versus* HSP60-treated mice on day 14; 14·4 ± 1·13% *versus* 10·9 ± 1·02% and *versus* 8·11 ± 0·74% in spleens, respectively, all $P < 0{\cdot}001$; 13·5 ± 1·05% *versus* 8·56 ± 0·64% and *versus* 9·91 ± 0·76% in CLNs, respectively, all $P < 0{\cdot}01$; Fig. 5e,h; Fig. 6e,h). Meanwhile, we also found that the frequency of Th17 cells in the spleens and CLNs of HSP60-treated mice on days 4 and 14 was lower than in those of untreated mice (untreated mice *versus* HSP60-treated mice on day 4 and *versus* HSP60-treated mice on day 14; 1·68 ± 0·13% *versus* 1·1 ± 0·09% and *versus* 0·67 ± 0·08% in spleens, respectively, all $P < 0{\cdot}001$; 1·36 ± 0·09% *versus* 0·69 ± 0·09% and *versus* 0·89 ± 0·08% in CLNs, respectively, all $P < 0{\cdot}001$; Fig. 5g,h, Fig. 6g,h). Additionally, our data showed that absolute numbers of Th1 and Th17 were decreased in the spleens and CLNs of HSP60-treated mice, respectively (Fig. 5i, Fig. 6i; all $P < 0{\cdot}01$). Unexpectedly, there were no significant differences in the frequency and number of Th2 cells in spleens and CLNs of HSP60-treated mice on days 4 and 14 compared with untreated mice (Fig. 5f,h,i, Fig. 6g–i).

Nasal HSP60 increases TGF-β and IL-10 secretion and decreases IFN-γ and IL-17 production in splenocytes

To determine the effect of the various T_{regs} induced by nasal HSP60 on the cytokine production profile from lymphocytes, we examined the cytokine levels in the supernatants of ConA-stimulated splenocytes on days 4 and 14 after the final nasal treatment using ELISA. There was a significant increase in TGF-β levels and an obvious decrease in the levels of IFN-γ and IL-17 in HSP60-treated mice on days 4 and 14 compared with untreated mice, respectively (Table 2, all $P < 0{\cdot}001$). Intriguingly, when compared with untreated mice, a marked up-regulation in IL-10 production was observed in HSP60-treated mice on day 14 (Table 2, $P < 0{\cdot}05$), but not on day 4. Moreover, we also examined cytokine production by splenocytes at 16 and 24 weeks, and a significant increase in TGF-β and IL-10 levels and a marked decrease in IFN-γ and IL-17 production was found in group II compared with group I (Table 2, all $P < 0{\cdot}05$). However, there were no significant differences in the levels of TGF-β, IL-10, IFN-γ and IL-17 between group III and groups IV or V (Table 2). Unfortunately, the levels of IL-4 were below the threshold of detection of the assay in all experiments.

Next, we determined the levels of cytokine mRNA expression by unstimulated splenocytes using real-time RT–PCR. Interestingly, a marked decrease in IFN-γ and IL-17 mRNA levels in HSP60-treated mice on days 4 (Fig. 7a, $P < 0{\cdot}05$) and 14 (Fig. 7a, $P < 0{\cdot}01$) were found than in untreated mice. Of note, there was a significant increase in TGF-β and IL-10 mRNA levels on day 14 and in mRNA TGF-β levels on day 4; however, the IL-4 mRNA levels were unchanged. Similarly, we observed increased TGF-β and IL-10 mRNA levels and decreased IFN-γ and IL-17 mRNA levels in group II compared with group I (Fig. 7b, all $P < 0{\cdot}05$). However, no differences were noticed in IL-4 mRNA levels between groups I and II. Additionally, up-regulated TGF-β mRNA levels were observed in groups IV and V compared with group III (Fig. 7c, $P < 0{\cdot}05$).

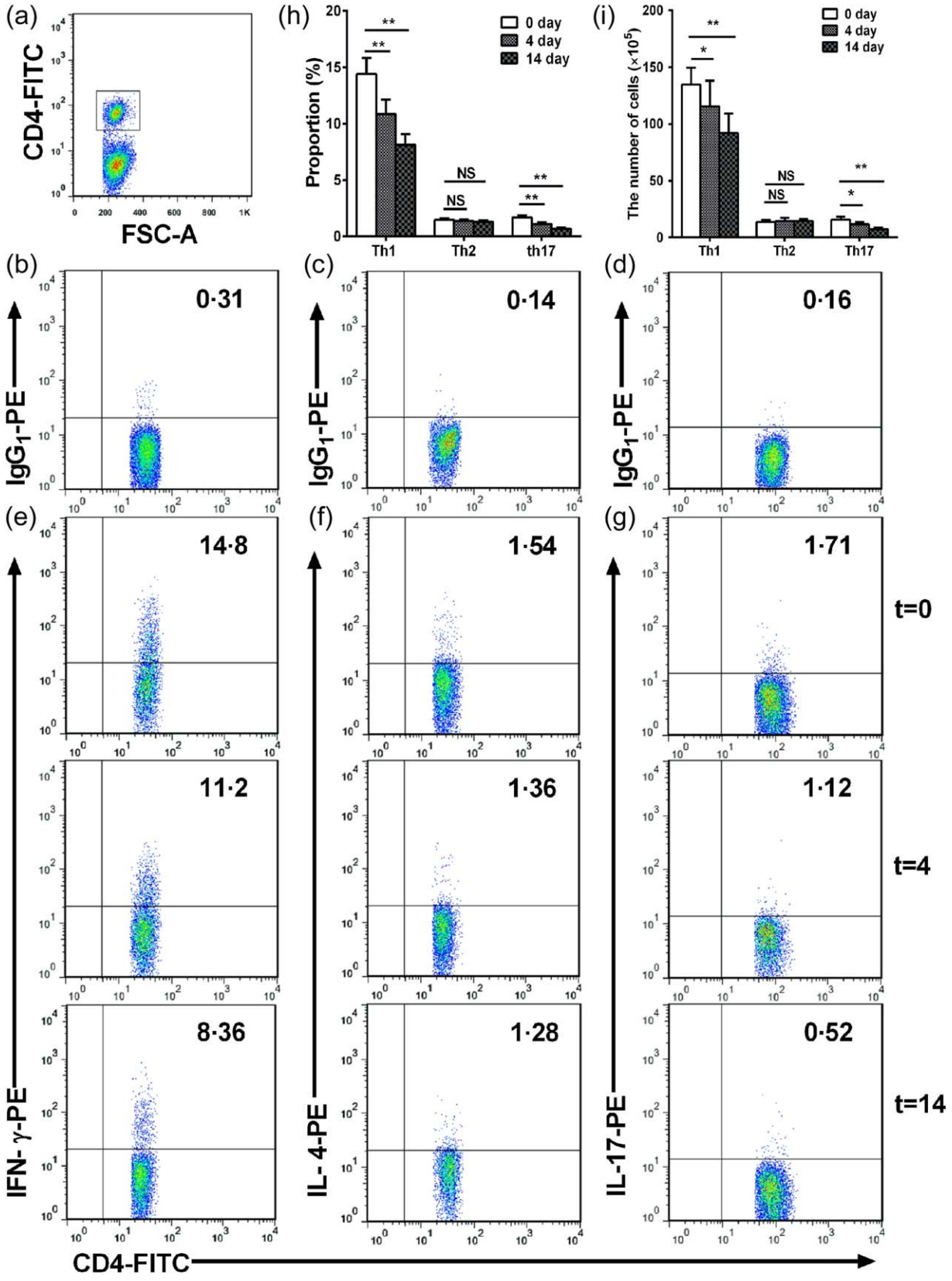

Fig. 5. Effects of nasal heat shock protein (HSP)60 on T helper type 1 (Th1), Th2 and Th17 cells in spleens. Apolipoprotein E (ApoE)$^{-/-}$ mice were administered HSP60 nasally for 5 days and were killed 4 and 14 days after the final nasal treatment. Untreated mice ($t = 0$) were considered controls. (a) CD4^{+} T cell subsets were gated. (b,d) Representative results for isotype controls in spleens estimated by fluorescence activated cell sorter (FACS) analysis. (e–g) Representative results for Th1 cells, Th2 cells and Th17 cells, respectively, in spleens estimated by FACS analysis. (h) The graphs represent the percentage of Th1, Th2 and Th17 cells in spleens, respectively. (i) The graphs represent the absolute number of Th1, Th2 and Th17 cells in spleens, respectively. *$P < 0{\cdot}05$, **$P < 0{\cdot}01$, and $^{n.s.}P > 0{\cdot}05$. The data are expressed as the mean ± standard error of the mean (s.e.m.) and are representative of at least three independent experiments.

Unexpectedly, IFN-γ, IL-4, IL-17, and IL-10 mRNA levels did not differ among groups III, IV and V.

The mRNA expression of T_{reg} markers and inflammatory markers in atherosclerotic lesions

To reveal whether nasal HSP60 affects the accumulation of T_{regs} and inflammatory cells in atherosclerotic lesions, we performed real-time RT–PCR analysis of TGF-β, CD25, FoxP3, IFN-γ, GARP and the adhesion molecules vascular cell adhesion protein 1 (VCAM-1) and monocyte chemotactic protein 1 (MCP-1) in thoracic aortas. Our data showed that TGF-β and FoxP3 mRNA expression were increased markedly, and the expression of IFN-γ, VCAM-1 and MCP-1 mRNA was reduced significantly in atherosclerotic lesions in group II compared with group I (Fig. 8a, all $P < 0{\cdot}05$). Unexpectedly, CD25 and GARP mRNA expression was similar in groups I and II. Notably, TGF-β and FoxP3 mRNA expression were increased markedly in group V compared with group III (Fig. 8b, $P < 0{\cdot}05$). In accordance with expectation, the expression levels of TGF-β and FoxP3 mRNA were unchanged in group IV compared with group III (Fig. 8b). Additionally, we found that the mRNA expression levels of the other cytokines did not differ significantly among groups III, IV and V (Fig. 8b).

Neutralizing anti-IL-10 antibody partly blocks the atheroprotective effect of nasal HSP60

Our finding showed that nasal HSP60 increased TGF-β and IL-10 production significantly. Our previous study found that a neutralizing anti-TGF-β-antibody increased atherosclerotic lesion formation significantly in HSP60-treated mice, suggesting that the atheroprotective effect of nasal HSP60 is partly dependent upon TGF-β [32]. However, whether IL-10 participates directly in inhibiting lesion formation following nasal HSP60 treatment remains uncertain. Therefore, an *in-vivo* IL-10 neutralization study was carried out using an anti-IL-10 antibody. As mentioned above, HSP60 was administered nasally to 6-week-old mice before the injection of neutralizing anti-IL-10-antibody (group VI) or control rat IgG (group VII). Our data revealed a significant increase (24·8%) in atherosclerotic lesion formation in group VI compared with group VII (Fig. 9; 353 437·2 ± 33 609·9 μm^2 *versus* 265 816·4 ± 26 705·3 μm^2; $P = 0{\cdot}003$), indicating that inhibiting IL-10 markedly increased atherosclerotic plaque formation.

Discussion

Emerging clinical and experimental facts have demonstrated that HSP60 plays an important role in atherosclerosis initiation and progression. Elevated plasma levels of soluble HSP60 and anti-HSP60 autoantibodies have been found in atherosclerotic patients and experimental atherosclerotic mice [26,27,40]. Autologous HSP60 can induce the generation of autoreactive HSP60-specific T cells and anti-HSP60 autoantibodies in ApoE$^{-/-}$ or LDLr$^{-/-}$ mice [41]. Furthermore, anti-HSP60 autoantibodies contribute to the development of atherosclerosis by accelerating endothelial damage and macrophage lysis [42,43]. In addition, HSP60-specific T cells have been observed in human atherosclerotic plaques and in atherosclerotic lesions in ApoE$^{-/-}$ mice, suggesting that HSP60-specific T cells are associated with early atherosclerotic events and terminating the HSP60-specific autoimmune response is known to be protective in atherosclerosis [28,44,45].

Previous studies have demonstrated clearly that the mucosal administration of autoantigens can be used to induce peripheral antigen-specific immune tolerance and to down-regulate antigen-specific T cells, eventually inhibiting excessive immune responses and helping to maintain self-tolerance to prevent autoimmune diseases [29–33,36]. Activated CD4^{+} T cells that are reactive to several antigens, including HSP60 and ox-LDL, mainly secrete a Th1-pattern of cytokines in atherosclerotic lesions, leading to an imbalance between Th1 and the T_{regs} specific for self- and non-self-antigens [46]. Restoring the balance between Th1 cells and T_{regs} may be effective in ameliorating atherosclerosis, suggesting that T_{regs} play a crucial role in controlling the initiation and progression of atherosclerosis [47]. Substantial studies have shown that HSP60 delivered via the oral and nasal route can induce immune tolerance successfully and increase the number of T_{regs}, which inhibit effector T cell responses by producing anti-inflammatory cytokines and attenuate the development of atherosclerosis [29,32]. The experimental results from our laboratory have revealed that the adoptive transfer of HSP60-specific T_{regs} to recombination-activating gene (RAG)$^{-/-}$ low-density lipoprotein receptor (LDLr)$^{-/-}$ mice can prevent the development of atherosclerosis [48]. Consequently, the above research suggested that the induction of mucosal tolerance and the subsequent activation of T_{regs} may be a novel and promising treatment approach for attenuating atherosclerosis.

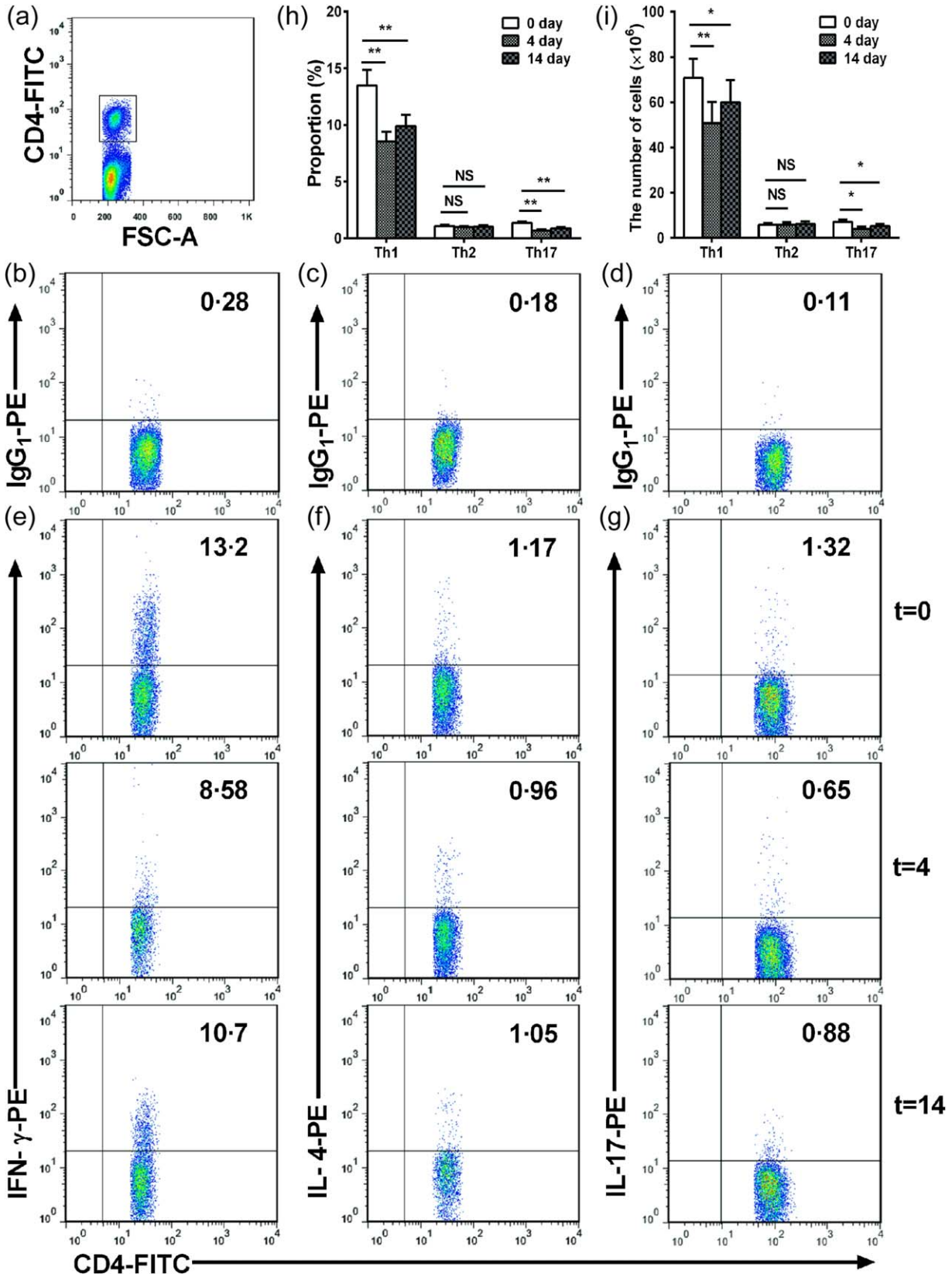

Fig. 6. Effects of nasal heat shock protein (HSP)60 on T helper type 1 (Th1), Th2 and Th17 cells in cervical lymph nodes (CLNs). Apolipoprotein E (ApoE)$^{-/-}$ mice were administered HSP60 nasally for 5 days and were killed 4 and 14 days after the final nasal treatment. Untreated mice ($t = 0$) were considered controls. (a) $CD4^+$ T cell subsets were gated. (b–d) Representative results for isotype controls in spleens estimated by fluorescence activated cell sorter (FACS) analysis. (e,g) Representative results for Th1 cells, Th2 cells and Th17 cells, respectively, in CLNs estimated by FACS analysis. (h), The graphs represent the percentage of Th1, Th2 and Th17 cells in CLNs, respectively. (i), The graphs represent the absolute number of Th1, Th2 and Th17 cells in CLNs, respectively. $^*P < 0{\cdot}05$, $^{**}P < 0{\cdot}01$ and $^{n.s.}P > 0{\cdot}05$. The data are expressed as the mean ± standard error of the mean (s.e.m.) and are representative of at least three independent experiments.

In the present study, we again found that nasal tolerance induction to a low dose of HSP60 suppressed early atherosclerosis significantly. This result is in line with previous studies from our laboratory and others, showing that nasal or oral tolerance induction to HSP60/65, β2-glycoprotein I and ox-LDL can reduce early atherosclerotic lesion formation [29–34,49]. In addition, this result is also supported by several lines of clinical observations, which indicate a more prominent role of HSP60-specific cellular immunity in the early stages of atherosclerosis [45,50]. However, our results are in agreement with studies showing that mucosal tolerance to self-antigens is not expected to inhibit advanced atherosclerosis [29,31]. Hence, we attempted to perform another experiment in group V, as mentioned above. Disappointingly, our data showed that the enhanced immunization once weekly led to only a mild but not significant reduction in lesion size during the progression of atherosclerosis. Nevertheless, our previous study demonstrated that an appropriate enhanced immune response to ox-LDL can contribute to attenuating atherosclerosis progression [33]. This discrepancy may be explained by the different types of antigens used in the above two studies. Therefore, further studies are required to identify a more effective method for reducing atherosclerosis progression via nasal HSP60.

It is well known that natural $CD4^+CD25^+FoxP3^+$ T_{regs}, which are the main population of T_{reg} subsets, exert suppressive effects in atherogenesis in mice [29,30,47]. In addition to naturally occurring T_{regs}, however, recent reports have shown that other types of T_{regs}, including Tr1, Th3 and $CD4^+LAP^+$ T cells, may be responsible for anti-atherosclerotic effects through the production of anti-inflammatory cytokines such as IL-10 and TGF-β [32–34]. Recently, GARP regulates the bioavailability and activation of TGF-β by binding to LAP on the cell surface [9,10,51]. Importantly, Wang *et al.* have demonstrated that αVβ6 and αVβ8 integrins are favoured to activate TGF-β from the GARP–proTGF-β1 complex, and cell-surface GARP contributed to this activation, suggesting that the GARP-proTGF-β1 complex could serve as a source of activated TGF-β1 [52]. Kalathil *et al.* has demonstrated recently that the number of $GARP^+FoxP3^+$ T_{regs} was increased significantly in patients with advanced hepatocellular carcinoma, and GARP expression was utilized to identify antigen-specific T_{regs} with high suppressive potential [53]. Moreover, our clinical investigations have shown that the frequency and function of $GARP^+$ T_{regs} were impaired in patients with acute coronary syndrome (ACS) [17,54,55]. These clinical findings suggested that $GARP^+$ T_{regs} may be involved in immune modulation of autoimmune and inflammatory diseases by producing immunosuppressive cytokines such as TGF-β. In the present study, our findings showed that nasal HSP60 increased the number of $CD4^+CD25^+GARP^+$ T_{regs} significantly, in particular activated $CD4^+CD25^+GARP^+$ T_{regs}, in spleens and CLNs on 4 days after nasal HSP60 treatment. More importantly, the influence lasted for at least 14 days. Although the suppressive function of $CD4^+CD25^+GARP^+$ T_{regs} remained unchanged nasal HSP60 led to a significant increase in TGF-β, which was secreted by $CD4^+CD25^+GARP^+$ T_{regs} in the spleens. This result is also supported by our clinical observations, which indicated that the TGF-β1 levels in the supernatants of cultured $GARP^+$ T_{regs} were reduced in ACS patients [17]. Similarly, we found a significant up-regulation of $CD4^+CD25^+FoxP3^+$ T_{regs} in the spleens and CLNs of HSP60-treated mice. To the best of our knowledge, this is the first report demonstrating a possible role for $CD4^+CD25^+GARP^+$ T_{regs} in the development of atherosclerosis in mice; however, further studies are required to offer more direct experimental support for the association between increased $CD4^+CD25^+GARP^+$ T_{regs} number or function and decreased atherosclerosis. In addition, whether or not $CD4^+CD25^+GARP^+$ T_{regs} can represent a new regulatory $CD4^+$ T cell phenotype that differs from other T_{reg} subtypes remains to be investigated.

Several studies have indicated that IL-10-secreting Tr1 cells have immunosuppressive properties, and these cells have been shown to play key roles in the development of Th1-mediated autoimmune diseases [56,57]. A decreased frequency of IL-10-producing Tr1 cells was observed in the inflamed synovium and peripheral blood of patients with rheumatoid arthritis, suggesting that a deficiency in Tr1 cells may play an important role in the loss of self-tolerance in autoimmune diseases [14,58]. Recently, Mallet *et al.* showed that adoptive transfer of Tr1 cells to ApoE$^{-/-}$ mice suppressed pathogenic Th1-mediated responses and reduced the development of atherosclerosis [16]. Interestingly, several studies have demonstrated that oral administration of self-antigens induces Tr1 cells that can inhibit multiple sclerosis and diabetes in animal models [59]. However, whether nasal administration of autoantigens can induce Tr1 cells is not entirely clear. In the current study,

Table 2. Cytokine production by concanavalin (ConA)-stimulated splenocytes

	Days after treatment							
				8 weeks		16 weeks		
	0 day ($n = 8$)	4 day (n = 6)	14 day $n = 7$)	Group I ($n = 6$)	Group II ($n = 6$)	Group III ($n = 6$)	Group IV ($n = 6$)	Group V ($n = 6$)
TGF-β_1	207·5 ± 19·5	380·3 ± 27·9*	448·3 ± 32·2*	192·8 ± 18·2	307·6 ± 26·1†	174·6 ± 16·4	187·1 ± 19	203·1 ± 19·7
IL-10	45·1 ± 11·7	51 ± 10·9	65·6 ± 11·3‡	57·8 ± 9·9	81·1 ± 13·5§	73·7 ± 13·1	79·2 ± 16·1	85·1 ± 12·9
IFN-γ	288·1 ± 19·9	267·5 ± 18·9*	251·5 ± 17·8*	318·5 ± 24·1	203·2 ± 19·4†	371·8 ± 36·2	382·5 ± 35·2	353·2 ± 23·3
IL-4	0	0	0	0	0	0	0	0
IL-17	29·6 ± 2·6	25·8 ± 1·7‡	20·9 ± 1·6*	41·6 ± 6·4	30·1 ± 4·7§	45·3 ± 8·6	43·2 ± 6·7	39·6 ± 7·4

*$P < 0{\cdot}001$ *versus* untreated mice; †$P < 0{\cdot}001$ *versus* group I; ‡$P < 0{\cdot}05$ *versus* untreated mice; §$P < 0{\cdot}05$ *versus* Group I. The data are expressed as the mean ± standard error of the mean (s.e.m.) and are representative of at least three independent experiments. Effects of nasal heat shock protein (HSP)60 on cytokine production in splenocytes. Apolipoprotein E (ApoE)$^{-/-}$ mice were administered phosphate-buffered saline (PBS) or HSP60 nasally for 5 days; untreated or PBS-treated mice were considered controls. Splenocytes collected from mice that were killed 4 and 14 days after the final nasal treatment, and at 16 and 24 weeks of age were stimulated with ConA *in vitro* for 72 h. Interferon (IFN)-γ, interleukin (IL)-4, IL-17, transforming growth factor (TGF)-β and IL-10 production in the supernatants was measured by enzyme-linked immunosorbent assay (ELISA).

we demonstrated that nasal administration of HSP60 can induce a marked increase in Tr1 cells in spleens and CLNs. This result is consistent with a study by Kilngenberg *et al.*, who reported that intranasal immunization with ApoB-100 attenuated atherosclerotic plaque formation by inducing an increased number of IL-10-producing Tr1 cells [34]. As the same time, we also found a significant decrease in Th1 and Th17 cells in the spleens and CLNs of HSP60-treated mice. These results demonstrated that nasal HSP60 can induce a shift from T helper cells towards T_{regs} in spleens and CLNs.

A substantial body of evidence indicates that TGF-β and IL-10 suppress autoimmune and inflammatory diseases, and IFN-γ and IL-17 are detrimental to many immunoinflammatory diseases [16,61,62]. TGF-β maintains the suppressor function of T_{regs} and inhibits the proliferation, activation and differentiation of $CD4^+$ T cells towards Th1, Th2, and Th17 in the periphery [63]. Previous studies have demonstrated that TGF-β or IL-10 deficiency increases atherosclerotic lesion formation in ApoE$^{-/-}$ mice [64,65]. In this study, our data showed that nasal HSP60 increases TGF-β and IL-10 production and decreases the secretion of IFN-γ and IL-17 in splenocytes. Simultaneously, we also observed a significant up-regulation of TGF-β and IL-10 mRNA levels and a marked down-regulation of IFN-γ and IL-17 mRNA levels in splenocytes in HSP60-treated mice. In addition, increased TGF-β and FoxP3 mRNA expression and decreased IFN-γ, VCAM-1 and MCP-1 mRNA expression were found in early lesions in HSP60-treated mice. Quite serendipitously, we did not observe a significant

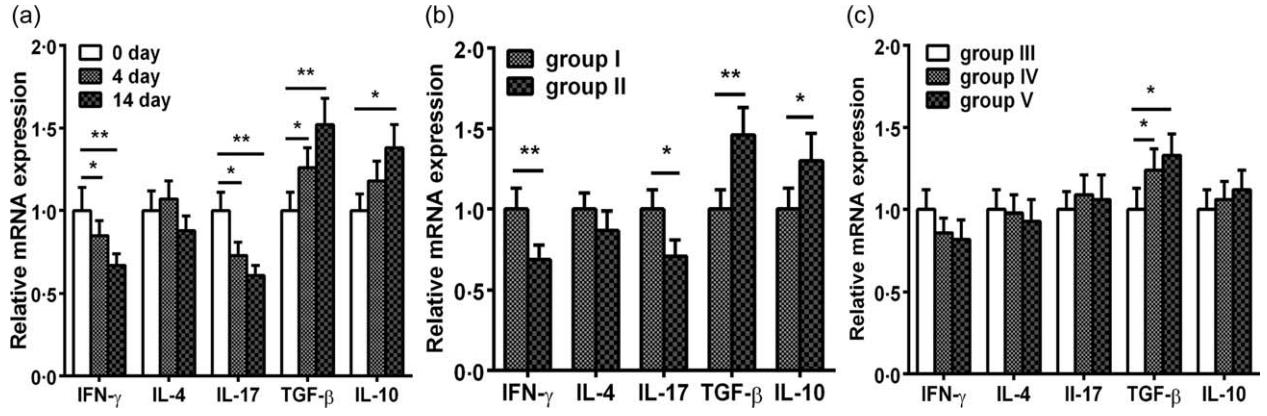

Fig. 7. Effects of nasal heat shock protein (HSP)60 on the relative expression of cytokine mRNA in splenocytes. Apolipoprotein E (ApoE)$^{-/-}$ mice were administered phosphate-buffered saline (PBS) or HSP60 nasally for 5 days; untreated or PBS-treated mice were considered controls. (a–c) Relative cytokine mRNA levels of interferon (IFN)-γ, interleukin (IL)-4, IL-17, transforming growth factor (TGF)-β and IL-10 in unstimulated splenocytes collected from mice that were killed 4 and 14 days after the final nasal treatment, and at 16 and 24 weeks of age were measured by real-time reverse transcription–polymerase chain reaction (RT–PCR). Fold change relative to PBS-treated mice is shown. *$P < 0{\cdot}05$, **$P < 0{\cdot}01$. The data are expressed as the mean ± standard error of the mean (s.e.m.) and are representative of at least three independent experiments.

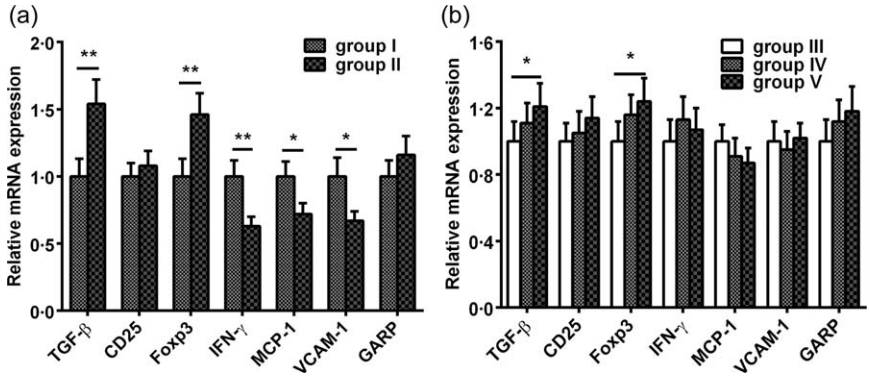

Fig. 8. Effects of nasal heat shock protein (HSP)60 on the relative mRNA expression of regulatory T cell markers and inflammatory markers in atherosclerotic plaques. (a,b) Total RNA was extracted from the aortas of 16- and 24-week-old phosphate-buffered saline (PBS)- or HSP60-treated mice. mRNA expression of regulatory T cell markers [transforming growth factor (TGF)-β, CD25, forkhead box transcription factor (FoxP3) and glycoprotein A repetitions predominant (GARP)] and inflammatory markers interferon (IFN)-γ, monocyte chemotactic protein (MCP)-1, vascular cell adhesion molecule (VCAM)-1 was determined quantitatively by real-time reverse transcription–polymerase chain reaction (RT–PCR). Fold-change relative to PBS-treated mice is shown. $^{*}P < 0{\cdot}05$, $^{**}P < 0{\cdot}01$. The data are expressed as the mean ± standard error of the mean (s.e.m.) and are representative of at least three independent experiments.

increase in GARP mRNA expression in lesions in HSP60-treated mice, possibly because there are other latent TGF-β-binding proteins in the plaques. Although IL-4 levels were unchanged in all groups, the differential effects of other inflammatory cytokines that were implicated previously in atherogenesis were again confirmed.

We and others have demonstrated previously that neutralizing anti-TGF-β antibodies reverse the suppressive function of T_{regs} in animal models of several autoimmune and inflammatory diseases, especially atherosclerosis [15,32,33,66]. In this study, in addition to a significant increase in TGF-β-producing T_{regs}, a noticeable up-regulation of IL-10-secreting Tr1 cells was also observed in HSP60-treated mice. It remains unknown, however, whether anti-IL-10 antibody treatment abrogates the suppressive effect of T_{regs}. We therefore performed a neutralizing anti-IL-10 antibody study and found that anti-IL-10 antibody treatment partly abolished the anti-atherosclerotic effects of nasal HSP60. This result is in concordance with several earlier studies describing that the suppressive effect of Tr1 cell clones on $CD4^+$ T cells was abrogated by neutralizing anti-IL-10 monoclonal antibodies [67,68]. Although we did not rule out the possible beneficial effect of nasal HSP60 on the humoral immune response due to a lack of detection of HSP60-specific antibodies, our study results support the possibility that nasal HSP60 inhibits atherosclerosis through an enhanced cellular immune response, including the induction of several types of T_{regs} and the production of TGF-β and IL-10.

In conclusion, we demonstrated that nasal tolerance induction to HSP60 inhibits early atherosclerotic lesion formation by inducing $CD4^+CD25^+GARP^+$ T_{regs}, Tr1 cells and $CD4^+CD25^+FoxP3^+$ T_{regs}, which produce large amounts of TGF-β and IL-10. Although further work is necessary to investigate the mechanism by which nasal HSP60 treatment increases T_{regs} and by which GARP regulates the activation of TGF-β, our results again confirm the fact that the induction of T_{regs} by nasal tolerance induction

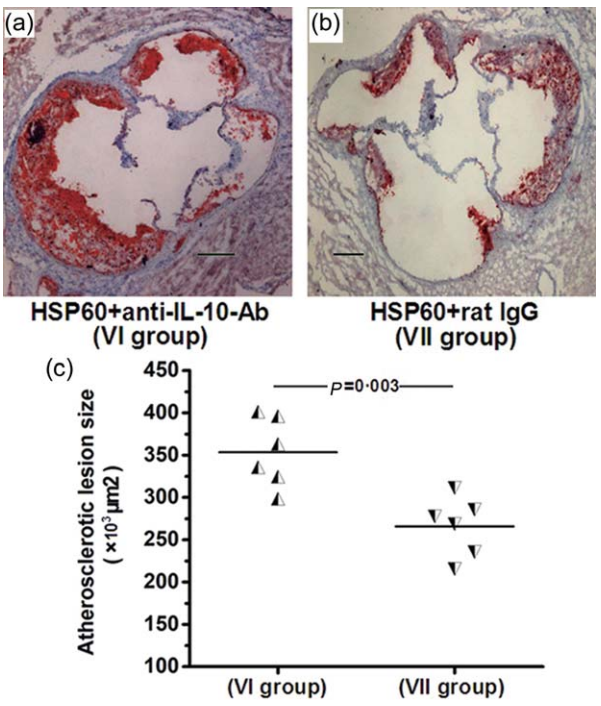

Fig. 9. Anti-atherosclerotic effect is partly interleukin (IL)-10 dependent. (a,b) Representative photomicrographs of oil red O- and haematoxylin-stained aortic root sections from the heat shock protein (HSP)60^+ anti-IL-10-antibody-treated group (VI, $n = 6$) and the $HSP60^+$ rat immunoglobulin (Ig)G-treated group (VII, $n = 6$). (c) The data from two groups are shown: the half black regular triangles represent animals from group VI and the half black inverted triangles represent animals from group VII. A black bar represents 200 μm. The horizontal bars represent the means.

to HSP60 could serve as a promising therapeutic method for treating atherosclerotic diseases.

Acknowledgements

This work was supported by grants from the National Natural Science Foundation of China (Nos. 81070237, 81270354, and 81300213)

Disclosure

The authors have no disclosures.

References

1 Fontenot JD, Gavin MA, Rudensky AY. Foxp3 programs the development and function of CD4+CD25+ regulatory T cells. Nat Immunol 2003; **4**:330–6.
2 Williams LM, Rudensky AY. Maintenance of the Foxp3-dependent developmental program in mature regulatory T cells requires continued expression of Foxp3. Nat Immunol 2007; **8**: 277–84.
3 Josefowicz SZ, Lu LF, Rudensky AY. Regulatory T cells: mechanisms of differentiation and function. Annu Rev Immunol 2012; **30**:531–64.
4 Allan SE, Crome SQ, Crellin NK *et al.* Activation-induced Foxp3 in human t effector cells does not suppress proliferation or cytokine production. Int Immunol 2007; **19**:345–54.
5 Wang J, Ioan-Facsinay A, van der Voort EI, Huizinga TW, Toes RE. Transient expression of Foxp3 in human activated nonregulatory $CD4^+$ T cells. Eur J Immunol 2007; **37**:129–38.
6 Roncarolo MG, Gregori S. Is FOXP3 a bona fide marker for human regulatory T cells? Eur J Immunol 2008; **38**:925–7.
7 Wang R, Wan Q, Kozhaya L, Fujii H, Unutmaz D. Identification of a regulatory T cell specific cell surface molecule that mediates suppressive signals and induces Foxp3 expression. PLOS ONE 2008; **3**:e2705.
8 Wang R, Kozhaya L, Mercer F, Khaitan A, Fujii H, Unutmaz D. Expression of GARP selectively identifies activated human FOXP3+ regulatory T cells. Proc Natl Acad Sci USA 2009; **106**:13439–44.
9 Tran DQ, Andersson J, Wang R, Ramsey H, Unutmaz D, Shevach EM. GARP (lrrc32) is essential for the surface expression of latent TGF-beta on platelets and activated $Foxp3^+$ regulatory T cells. Proc Natl Acad Sci USA 2009; **106**:13445–50.
10 Stockis J, Colau D, Coulie PG, Lucas S. Membrane protein GARP is a receptor for latent TGF-beta on the surface of activated human Treg. Eur J Immunol 2009; **39**:3315–22.
11 Probst-Kepper M, Geffers R, Kroger A *et al.* GARP: a key receptor controlling foxp3 in human regulatory T cells. J Cell Mol Med 2009; **13**:3343–57.
12 Stephens LA, Gray D, Anderton SM. $CD4^+CD25^+$ regulatory T cells limit the risk of autoimmune disease arising from T cell receptor cross reactivity. Proc Natl Acad Sci USA 2005; **102**: 17418–23.
13 Wu HY, Center EM, Tsokos GC, Weiner HL. Suppression of murine SLE by oral anti-CD3: inducible $CD4^+CD25^-LAP^+$ regulatory T cells control the expansion of $IL\text{-}17^+$ follicular helper T cells. Lupus 2009; **18**:586–96.
14 Yudoh K, Matsuno H, Nakazawa F, Yonezawa T, Kimura T. Reduced expression of the regulatory CD4+ T cell subset is related to Th1/Th2 balance and disease severity in rheumatoid arthritis. Arthritis Rheum 2000; **43**:617–27.
15 Sasaki N, Yamashita T, Takeda M *et al.* Oral anti-CD3 antibody treatment induces regulatory T cells and inhibits the development of atherosclerosis in mice. Circulation 2009; **120**:1996–2005.
16 Mallat Z, Gojova A, Brun V *et al.* Induction of a regulatory T cell type 1 response reduces the development of atherosclerosis in apolipoprotein E-knockout mice. Circulation 2003; **108**: 1232–7.
17 Meng K, Zhang W, Zhong Y *et al.* Impairment of circulating $CD4^+CD25^+GARP^+$ regulatory T cells in patients with acute coronary syndrome. Cell Physiol Biochem 2014; **33**:621–32.
18 Wick G, Kleindienst R, Dietrich H, Xu Q. Is atherosclerosis an autoimmune disease? Trends Food Sci Technol 1992; **3**:114–9.
19 Packard RR, Lichtman AH, Libby P. Innate and adaptive immunity in atherosclerosis. Semin Immunopathol 2009; **31**:5–22.
20 Galkina E, Ley K. Immune and inflammatory mechanisms of atherosclerosis. Annu Rev Immunol 2009; **27**:165–97.
21 Wick G, Jakic B, Buszko M, Wick MC, Grundtman C. The role of heat shock proteins in atherosclerosis. Nat Rev Cardiol 2014; **11**:516–29.
22 Alard JE, Dueymes M, Youinou P, Jamin C. Modulation of endothelial cell damage by anti-Hsp60 autoantibodies in systemic autoimmune diseases. Autoimmun Rev 2007; **6**:438–43.
23 Cappello F, Conway de Macario E, Di Felice V, Zummo G, Macario AJ. *Chlamydia trachomatis* infection and anti-Hsp60 immunity: the two sides of the coin. PLOS Pathog 2009; **5**: e1000552
24 Jang EJ, Jung KY, Hwang E, Jang YJ. Characterization of human anti-heat shock protein 60 monoclonal autoantibody Fab fragments in atherosclerosis: genetic and functional analysis. Mol Immunol 2013; **54**:338–46.
25 Kleindienst R, Xu Q, Willeit J, Waldenberger FR, Weimann S, Wick G. Immunology of atherosclerosis. Demonstration of heat shock protein 60 expression and T lymphocytes bearing alpha/beta or gamma/delta receptor in human atherosclerotic lesions. Am J Pathol 1993; **142**:1927–37.
26 Xu Q, Schett G, Perschinka H *et al.* Serum soluble heat shock protein 60 is elevated in subjects with atherosclerosis in a general population. Circulation 2000; **102**:14–20.
27 Zhang X, He M, Cheng L *et al.* Elevated heat shock protein 60 levels are associated with higher risk of coronary heart disease in Chinese. Circulation 2008; **118**:2687–93.
28 Almanzar G, Öllinger R, Leuenberger J *et al.* Autoreactive HSP60 epitope-specific T-cells in early human atherosclerotic lesions. J Autoimmun 2012; **39**:441–50.
29 van Puijvelde GH, van Es T, van Wanrooij EJ *et al.* Induction of oral tolerance to HSP60 or an HSP60-peptide activates T cell regulation and reduces atherosclerosis. Arterioscler Thromb Vasc Biol 2007; **27**:2677–83.
30 van Puijvelde GH, Hauer AD, de Vos P *et al.* Induction of oral tolerance to oxidized low-density lipoprotein ameliorates atherosclerosis. Circulation 2006; **114**:1968–76.
31 George J, Yacov N, Breitbart E *et al.* Suppression of early atherosclerosis in LDL-receptor deficient mice by oral tolerance with beta 2-glycoprotein I. Cardiovasc Res 2004; **62**:603–9.

32 Li H, Ding Y, Yi G, Zeng Q, Yang W. Establishment of nasal tolerance to heat shock protein-60 alleviates atherosclerosis by inducing TGF-β-dependent regulatory T cells. J Huazhong Univ Sci Technolog Med Sci 2012; **32**:24–30.

33 Zhong Y, Wang X, Ji Q *et al.* $CD4^+LAP^+$ and $CD4^+CD25^+Foxp3^+$ regulatory T cells induced by nasal oxidized low-density lipoprotein suppress effector T cells response and attenuate atherosclerosis in $ApoE^{-/-}$ mice. J Clin Immunol 2012; **32**:1104–17.

34 Klingenberg R, Lebens M, Hermansson A *et al.* Intranasal immunization with an apolipoprotein B-100 fusion protein induces antigen-specific regulatory T cells and reduces atherosclerosis. Arterioscler Thromb Vasc Biol 2010; **30**:946–52.

35 Ma CG, Zhang GX, Xiao BG, Link J, Olsson T, Link H. Suppression of experimental autoimmune myasthenia gravis by nasal administration of acetylcholine receptor. J Neuroimmunol 1995; **58**:51–60.

36 Maron R, Sukhova G, Faria AM *et al.* Mucosal administration of heat shock protein-65 decreases atherosclerosis and inflammation in aortic arch of low-density lipoprotein receptor-deficient mice. Circulation 2002; **106**:1708–15.

37 Lu H, Wagner WM, Gad E *et al.* Treatment failure of a TLR-7 agonist occurs due to self-regulation of acute inflammation and can be overcome by IL-10 blockade. J Immunol 2010; **184**: 5360–7.

38 Wolvers DA, Coenen-de Roo CJ, Mebius RE *et al.* Intranasally induced immunological tolerance is determined by Characteristics of the draining lymph nodes: studies with OVA and human cartilage gp-39. J Immunol 1999; **162**:1994–8.

39 Ding Q, Lu L, Wang B *et al.* B7H1-Ig fusion protein activates the $CD4^+$ IFN-gamma $receptor^+$ type 1 T regulatory subset through IFN-gamma-secreting Th1 cells. J Immunol 2006; **177**: 3606–14.

40 Mandal K, Foteinos G, Jahangiri M, Xu Q. Role of antiheat shock protein 60 autoantibodies in atherosclerosis. Lupus 2005; **14**:742–6.

41 Grundtman C, Kreutmayer SB, Almanzar G, Wick MC, Wick G. Heat shock protein 60 and immune inflammatory responses in atherosclerosis. Arterioscler Thromb Vasc Biol 2011; **31**:960–8.

42 Foteinos G, Afzal AR, Mandal K, Jahangiri M, Xu Q. Anti-heat shock protein 60 autoantibodies induce atherosclerosis in apolipoprotein E-deficient mice via endothelial damage. Circulation 2005; **112**:1206–13.

43 Schett G, Metzler B, Mayr M *et al.* Macrophage-lysis mediated by autoantibodies to heat shock protein 65/60. Atherosclerosis 1997; **128**:27–38.

44 Curry AJ, Portig I, Goodall JC, Kirkpatrick PJ, Gaston JS. T lymphocyte lines isolated from atheromatous plaque contain cells capable of responding to Chlamydia antigens. Clin Exp Immunol 2000; **121**:261–9.

45 Knoflach M, Kiechl S, Mayrl B *et al.* T-cell reactivity against HSP60 relates to early but not advanced atherosclerosis. Atherosclerosis 2007; **195**:333–8.

46 Mallat Z, Ait-Oufella H, Tedgui A. Regulatory T cell responses: potential role in the control of atherosclerosis. Curr Opin Lipidol 2005; **16**:518–24.

47 Ait-Oufella H, Salomon BL, Potteaux S *et al.* Natural regulatory T cells control the development of atherosclerosis in mice. Nat Med 2006; **12**:178–80.

48 Yang K, Li D, Luo M, Hu Y. Generation of HSP60-specific regulatory T cell and effect on atherosclerosis. Cell Immunol 2006; **243**:90–5.

49 Xiong Q, Li J, Jin L, Liu J, Li T. Nasal immunization with heat shock protein 65 attenuates atherosclerosis and reduces serum lipids in cholesterol-fed wild-type rabbits probably through different mechanisms. Immunol Lett 2009; **125**:40–5.

50 Knoflach M, Kiechl S, Penz D *et al.* Cardiovascular risk factors and atherosclerosis in young women: atherosclerosis risk factors in female youngsters (ARFY study). Stroke 2009; **40**: 1063–9.

51 Gauthy E, Cuende J, Stockis J *et al.* GARP is regulated by miRNAs and controls latent TGF-β1 production by human regulatory T cells. PLOS ONE 2013; **8**:e76186

52 Wang R, Zhu J, Dong X, Shi M, Lu C, Springer TA. GARP regulates the bioavailability and activation of TGF-β. Mol Biol Cell 2012; **23**:1129–39.

53 Kalathil S, Lugade AA, Miller A, Iyer R, Thanavala Y. Higher frequencies of GARP(+) CTLA-4(+)Foxp3(+) T regulatory cells and myeloid-derived suppressor cells in hepatocellular carcinoma patients are associated with impaired T-cell functionality. Cancer Res 2013; **73**:2435–44.

54 Zhu ZF, Meng K, Zhong YC *et al.* Impaired circulating CD4+ LAP+ regulatory T cells in patients with acute coronary syndrome and its mechanistic study. PLOS ONE 2014; **9**:e88775

55 Liu Y, Zhao X, Zhong Y *et al.* Heme oxygenase-1 restores impaired $GARPCD4^+CD25^+$ regulatory T cells from patients with acute coronary syndrome by upregulating LAP and GARP expression on activated T lymphocytes. Cell Physiol Biochem 2015; **35**:553–70.

56 Groux H, O'Garra A, Bigler M *et al.* A $CD4^+$ T-cell subset inhibits antigen-specific T-cell responses and prevents colitis. Nature 1997; **389**:737–42.

57 Lou W, Wang C, Wang Y, Han D, Zhang L. Enhancement of the frequency and function of IL-10-secreting type I T regulatory cells after 1 year of cluster allergen-specific immunotherapy. Int Arch Allergy Immunol 2012; **159**:391–8.

58 Han D, Wang C, Lou W, Gu Y, Wang Y, Zhang L. Allergen-specific IL-10-secreting type I T regulatory cells, but not CD4(+)CD25(+)Foxp3(+) T cells, are decreased in peripheral blood of patients with persistent allergic rhinitis. Clin Immunol 2010; **136**:292–301.

59 Battaglia M, Gianfrani C, Gregori S, Roncarolo MG. IL-10-producing T regulatory type 1 cells and oral tolerance. Ann NY Acad Sci 2004; **1029**:142–53.

60 Bettini M, Vignali DA. Regulatory T cells and inhibitory cytokines in autoimmunity. Curr Opin Immunol 2009; **21**: 612–8.

61 Shabgah AG, Fattahi E, Shahneh FZ. Interleukin-17 in human inflammatory diseases. Postepy Dermatol Alergol 2014; **31**:256–61.

62 Rizza P, Moretti F, Belardelli F. Recent advances on the immunomodulatory effects of IFN-alpha: implications for cancer immunotherapy and autoimmunity. Autoimmunity 2010; **43**: 204–9.

63 Mantel PY, Schmidt-Weber CB. Transforming growth factor-beta: recent advances on its role in immune tolerance. Methods Mol Biol 2011; **677**:303–38.

64 Mallat Z, Gojova A, Marchiol-Fournigault C *et al.* Inhibition of transforming growth factor-beta signaling accelerates atherosclerosis and induces an unstable plaque phenotype in mice. Circ Res 2001; **89**:930–4.
65 Caligiuri G, Rudling M, Ollivier V *et al.* Interleukin-10 deficiency increases atherosclerosis, thrombosis, and low-density lipoproteins in apolipoprotein E knockout mice. Mol Med 2003; **9**:10–7.
66 Powrie F, Carlino J, Leach MW, Mauze S, Coffman RL. A critical role for transforming growth factor-beta but not interleukin 4 in the suppression of T helper type 1-mediated colitis by CD45RB(low) $CD4^+$ T cells. J Exp Med 1996; **183**: 2669–74.
67 Groux H, Bigler M, de Vries JE, Roncarolo MG. Interleukin-10 induces a long-term antigen-specific anergic state in human $CD4^+$ T cells. J Exp Med 1996; **184**:19–29.
68 Hunter MM, Wang A, Hirota CL, McKay DM. Neutralizing anti-IL-10 antibody blocks the protective effect of tapeworm infection in a murine model of chemically induced colitis. J Immunol 2005; **174**:7368–75.

Supporting information

Additional Supporting information may be found in the online version of this article at the publisher's web-site:

Fig. S1. Nasal heat shock protein (HSP)60 fails to inhibit atherosclerotic lesion progression. (a–c) Representative photomicrographs of oil red O- and haematoxylin-stained aortic root sections from the control-treated group (III, $n = 6$), the HSP60-treated group (IV, $n = 6$) and the HSP60-treated enhancement group (V, $n = 6$). (d) The data from three groups are shown: the half black regular triangles, the half black inverted triangles and the black inverted triangles represent animals from groups III, IV and V. A black bar represents 200 μm. The horizontal bars represent the means.

Fig. S2. Effects of nasal heat shock protein (HSP)60 on the suppressive function of $CD4^+CD25^+$ glycoprotein A repetitions predominant $(GARP)^+$ regulatory T cells (T_{regs}). $CD4^+CD25^+GARP^+$ T_{regs} and $CD4^+CD25^-GARP^-$ T cells were isolated from spleens 14 days after the final nasal HSP60 treatment. $CD4^+CD25^+GARP^+$ T_{regs} from phosphate-buffered saline (PBS)-treated or HSP60-treated mice were co-cultured with $CD4^+CD25^-GARP^-$ T cells at different ratios in the presence of soluble anti-CD3-antibody and anti-CD28-antibody. Cell proliferation was assessed using the MTT assay. The rate of cell proliferation was calculated as follows: cell proliferation rate = (A value in test group − A value in normal control group)/A value in normal control group × 100%. The data are representative of at least three independent experiments.

Table S1. Apolipoprotein E $(ApoE)^{-/-}$ mice were nasally administered phosphate-buffered saline (PBS) or heat shock protein (HSP)60, as described in the Methods section. The data are expressed as the mean ± standard error of the mean (s.e.m.).